



UNIVERSITEIT•STELLENBOSCH•UNIVERSITY
jou kennisvenoot • your knowledge partner

*Comparison of Three Prototype Flux -Modulating Permanent Magnet Machines
(repository copy)*

Article:

Gerber, S., Wang, R-J., (2018) Comparison of three prototype flux-modulating permanent magnet machines, *XXIII International Conference on Electrical Machines*, (ICEM), pp. 2072--2078, 3-6 September 2018, Alexandroupoli, Greece

<http://dx.doi.org/10.1109/ICELMACH.2018.8506736>

Reuse

Unless indicated otherwise, full text items are protected by copyright with all rights reserved. Archived content may only be used for academic research.

Comparison of Three Prototype Flux-Modulating Permanent Magnet Machines

Stiaan Gerber and Rong-Jie Wang

Abstract—In recent years, many interesting machine topologies based on the flux-modulation principle have been proposed. An attractive feature of these machines is the high torque density that can be realized. Many works in this field highlight the merits of a single topology. In this paper, the performances and material requirements of several different flux-modulating machines that have been optimized within the same constraints are compared in detail. Some experimental results are highlighted and the operational ranges of the machines are presented. A conventional fractional-slot PM machine with a non-overlap winding is included in the comparison as a benchmark. The machine topologies featuring a full magnetic gear achieve the highest torque, but their mechanical complexity is high. The vernier machine can achieve high torque at low speeds and has a wide constant power speed range, but its power factor is poor when delivering high torque. The flux-modulating machines outperform the benchmark machine in terms of torque density and efficiency.

Index Terms—Design optimization, finite element analysis, gears, performance evaluation, permanent magnet machines, rotating machines

I. INTRODUCTION

IN recent years, many interesting machines based on the flux-modulation principle employed in some magnetic gears have been proposed [1]–[7]. Different methods of integrating a magnetic gear and an electrical machine into a single entity, here referred to as a magnetically geared machine, have been investigated. Also, in the process of seeking alternatives that are simpler from a mechanical construction perspective, machines such as vernier machines have received renewed attention [8]–[10]. The main driver behind the interest in these machines has been the promise of superior torque density and high efficiency when compared with more conventional permanent magnet (PM) machines.

Over the course of a few years, several small prototypes with similar design constraints have been developed as part of a research project on flux-modulating electrical machines. The goal was to investigate the feasibility of these machines and to test if their advantages can be realized. In this paper, the electromagnetic performances of these prototypes are compared in detail. The work builds on the comparison presented in [11] which was made prior to the realization of

TABLE I
DESIGN SPECIFICATIONS

Parameter	Value
Outer diameter	140 mm
Stack length	50 mm
Air-gap length	0.7 mm
Current density	5 A/mm ²
Winding fill factor	0.55

any prototypes. A conventional fractional-slot PM machine with a non-overlap winding is also designed and used as a benchmark in the comparison. Cross-sectional views of the benchmark machine and the three flux-modulating machines are shown in Fig. 1.

The content of the paper is structured as follows: In section II, the design procedure and constraints applied to each prototype is described. Section III compares some experimental results from the different prototypes, while in section IV, a detailed comparison of the machines' performance characteristics, material requirements and operational ranges is presented. Conclusions are drawn in section V.

II. DESIGN

The design of each machine shown in Fig. 1 is briefly discussed in this section. Previous works have described the design and evaluation of each prototype in detail. All machines were optimized to achieve maximum torque, within the specifications of Table I. Thus, fixed volume optimizations were performed. All machines employed NdFeB magnets, grade N48H.

The design analyses were based on 2D finite element method (FEM) simulations and gradient-based optimization algorithms were employed with multiple initial design points.

A. Direct-drive Machine

The first machine is a conventional fractional-slot PM machine with a non-overlap winding, referred to as the direct-drive machine (DDM) in this paper. This design was used as a benchmark in this study. The geometric design variables considered in the optimization are illustrated in Figs. 2a and 2b. In addition, several pole/slot combinations were considered. Detailed design parameters can be found in [12].

B. Split MGM

The second machine is referred to as a split magnetically geared machine (SMGM), described in [13]. It consists of four concentric components with three air gaps. A special

This work was supported in part by the National Research Foundation of South Africa and ABB Corporate Research, Sweden.

S. Gerber and R-J. Wang are with the Department of Electrical and Electronic Engineering, Stellenbosch University, Stellenbosch, 7600, South Africa (e-mail: sgerber@sun.ac.za, rwang@sun.ac.za)

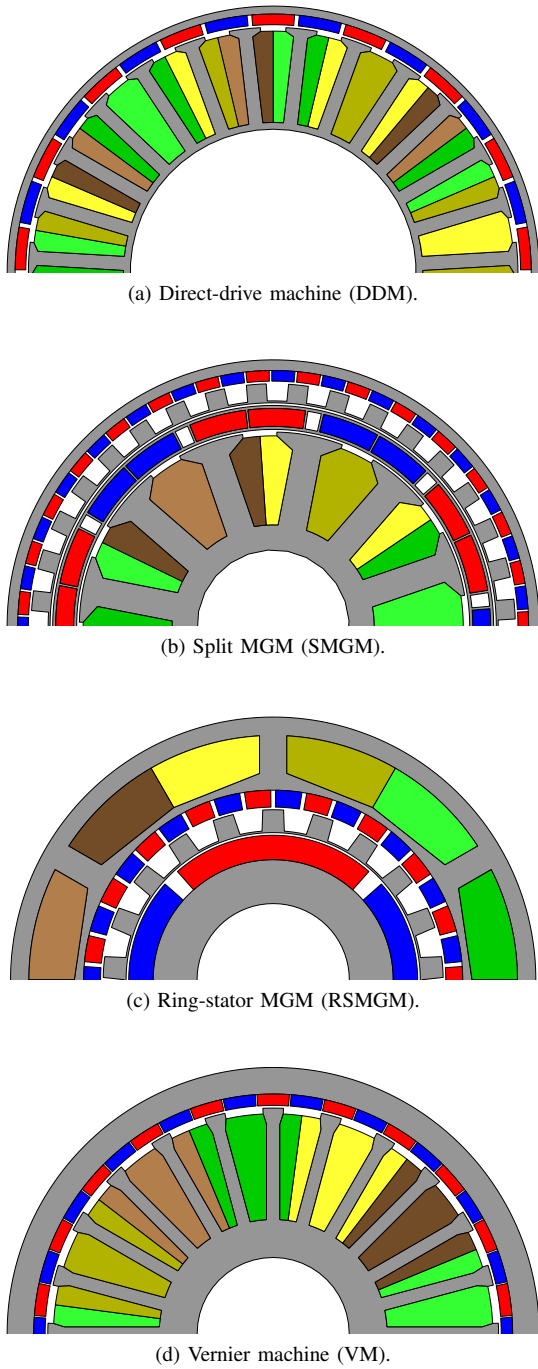


Fig. 1. Machine topologies considered in this paper.

laminated carrier was used to house the magnets of the sun gear (high-speed rotor). The geometric design variables for this machine are shown in Figs. 2a - 2d.

In the optimization process, the gear and machine components were well matched by constraining the stator load factor, as described in [13].

After initial optimization, the sun gear cogging torque was minimized by varying the stator slot opening. This approach was sufficient to reduce cogging to an acceptable level.

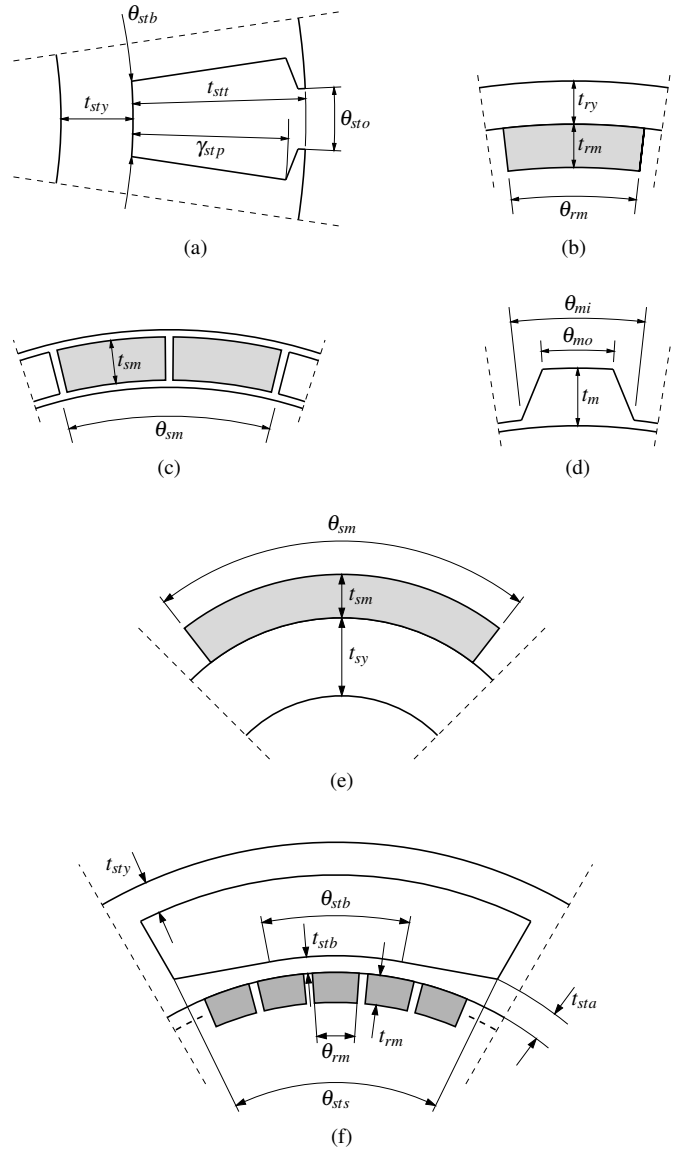


Fig. 2. Optimization design variables.

C. Ring-stator MGM

The third machine is referred to as a ring-stator magnetically geared machine (RSMGM). Details on the design can be found in [14]. The topology is also called a *pseudo direct-drive machine* [2]. It consists of three concentric components. The ring gear magnets are fixed to the inner surface of the stator. Figs. 2d - 2f show the geometric design variables considered for this machine.

The optimization of this machine also made use of the stator load factor concept to ensure appropriate torque capability of the gear and machine components, respectively.

D. Vernier Machine

The fourth machine is a PM vernier machine (VM), presented in [12]. Unlike the other topologies considered here, the vernier machine has an overlap winding. It is interesting to note that this is the only fundamental difference

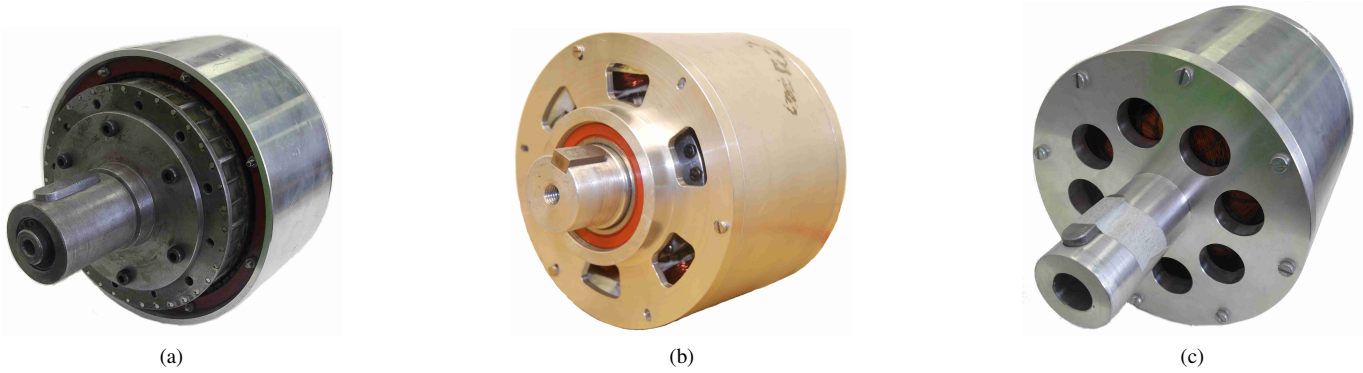


Fig. 3. Prototype machines. (a) Split MGM. (b) Ring-stator MGM. (c) Vernier machine

between the vernier machine and the direct-drive machine. The geometrical design variables for this machine are the same as that of the direct-drive machine, shown in Figs. 2a and 2b. Various gear ratios and pole/slot combinations were considered.

III. PERFORMANCE EVALUATION

In this section, some simulation and experimental results achieved with the three prototype machines are highlighted. The prototypes are shown in Fig. 3.

A. Split MGM

Simulated and measured no-load line voltage waveforms are compared in Fig. 4 and can be seen to be in good agreement.

The machine was tested at different speeds and loads in generator mode by connecting the output to a resistive load. The measured efficiency map for the split MGM is shown in Fig. 5.

The gear component of the prototype achieved a stall torque of 82 Nm, while 3D FEM predicted a value of 88 Nm.

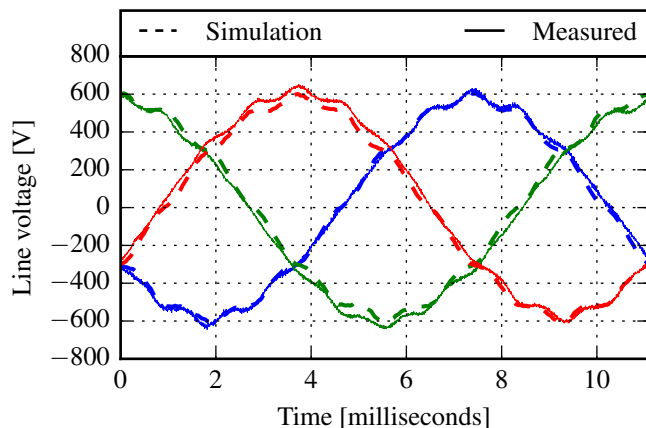


Fig. 4. Comparison of measured and simulated split MGM line voltage waveforms.

B. Ring-stator MGM

A comparison between simulated and measured no-load line voltage waveforms is shown in Fig. 6. The waveforms contain a significant 5th harmonic and has the highest total harmonic distortion of the three prototypes.

The ring-stator MGM was tested in generator mode driving a resistive load. The efficiency of the prototype was compromised because the fill factor achieved was significantly lower than the design value. An efficiency map of the prototype is shown in Fig. 7.

This prototype achieved a stall torque of 59 Nm, which is very close to the 61 Nm predicted by 3D FEM.

C. Vernier Machine

The vernier machine exhibited very low cogging torque and the no-load line voltage waveforms, shown in Fig. 8 are nearly perfectly sinusoidal. The PM excitation in the vernier machine provides limited exciting flux. The machine requires reactive power in order to produce its rated torque. For this reason, the machine was tested in generator mode using a variable RC load. A measured efficiency map is shown in Fig. 9. In general, the measured efficiency was lower than the optimized design value due to the lower fill factor of the prototype.

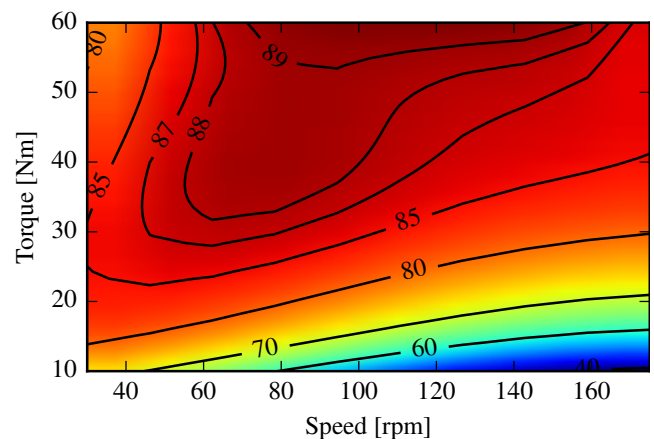


Fig. 5. Measured efficiency map of the Split MGM prototype.

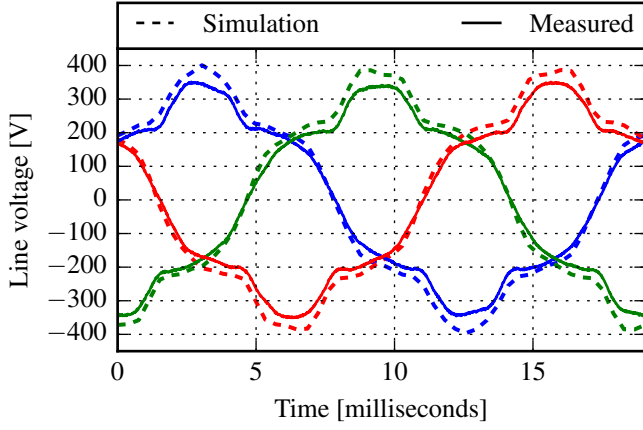


Fig. 6. Comparison of measured and simulated ring-stator MGM line voltage waveforms.

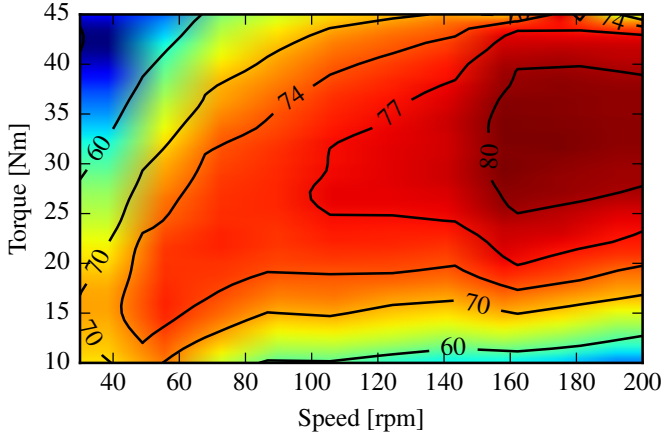


Fig. 7. Measured efficiency map of the Ring-stator MGM prototype.

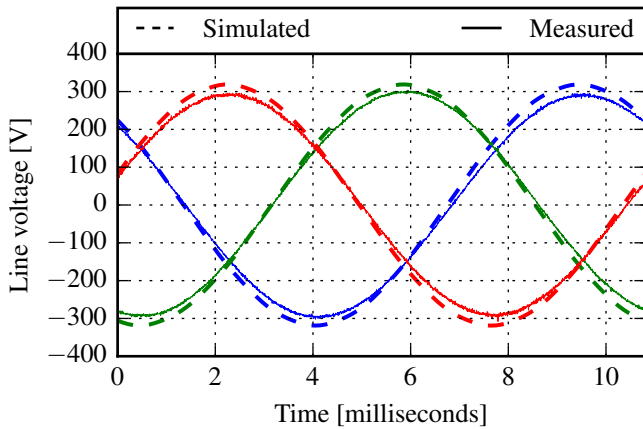


Fig. 8. Comparison of measured and simulated vernier machine line voltage waveforms.

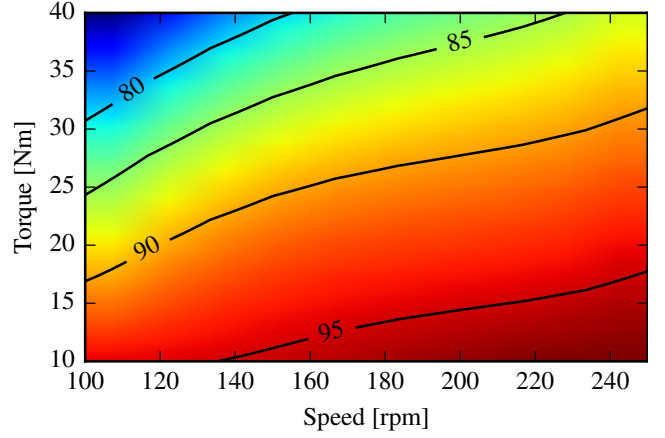


Fig. 9. Measured efficiency map of the Vernier machine prototype.

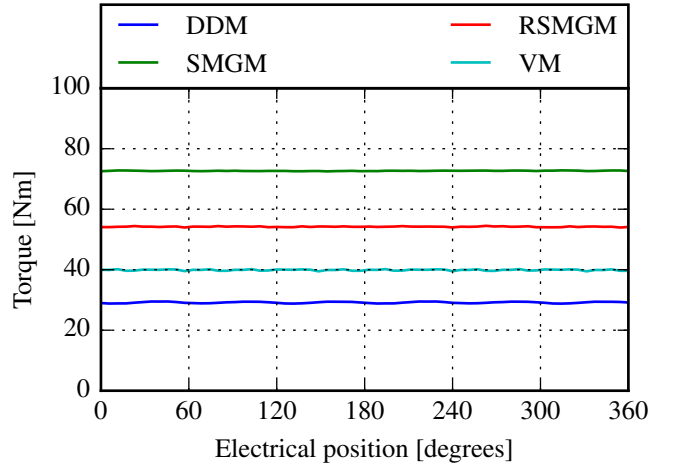


Fig. 10. Comparison of simulated full load torque waveforms.

D. Torque Performance

Fig. 10 shows a comparison of the simulated torque waveforms of the optimized machines. Clearly, all the machines considered in this study have smooth torque transfer characteristics.

IV. COMPARISON OF MACHINE TOPOLOGIES

In this section, the prototypes that have been constructed and the benchmark direct-drive machine are compared in detail, including performance characteristics and material requirements.

A. Rated Performance Characteristics

Table II shows a comparison of the various designs (Fig. 1) considered in this study, including the benchmark direct-drive machine (DDM), split MGM (SMGM), the ring-stator MGM (RSMGM) and the vernier machine (VM).

For the MGMs, the stall torque was obtained from 3D FEM. The table also lists their respective end-effect ratios (E_T), [15]. All other calculations, including the MGM stator torques and the torque of the DDM and the VM are based

on 2D simulation data, together with parameters that account for the end-windings. The dq end-winding inductances were calculated by subtracting the inductance calculated with 2D FEM from that calculated with 3D FEM. The calculated copper loss includes the contribution of the end-winding and is based on a copper fill factor of 0.55 for all machines. In the table, the end-winding factor indicates the length of the end-windings relative to the stack length, for each machine. Magnet loss and core loss data are based on transient 2D FEM.

The SMGM achieved the highest rated torque, torque density and torque per active mass. Its rated torque density is 2.7 times higher than the DDM. The RSMGM also has a very high torque density. Although the VM's torque per active mass is lower than that of the DDM, its torque per volume is almost 1.5 times higher.

The rated copper loss of the SMGM is the lowest. Even though the rated stator torque of the RSMGM is the lowest, its rated copper loss is similar to that of the DDM and the VM. The copper loss in the DDM is very high, considering that its rated torque is lower than that of the other machines. This is despite the fact that the DDM has the shortest end-windings. Despite the long end-windings of the VM, its copper loss is not excessively high.

In all the machines, the losses generated in the magnets are small compared to the copper loss and the core loss. The DDM has very low magnet loss. The magnet loss of the two MGMs are the highest. Note that the magnet loss of the SMGM would have been much higher if not for the magnet carrier design employed for the sun gear, as described in [13].

The core loss of the DDM is the lowest, whereas the SMGM has the highest core loss. The RSMGM and the VM also have low core loss. The reason for the high core loss in the SMGM is its high operating frequency, compared to the other machines. This machine's operating frequency is higher than the other machines because it was the only machine that benefited from a higher pole count within the specified volume. For the other machines, a higher pole count did not result in a significant increase in maximum torque.

The efficiency of the SMGM is the highest. The reference DDM has a poor efficiency due to its high copper loss and relatively low torque.

Among these machines, the VM is the only one with a poor power factor.

The MGMs used more than double the amount of permanent magnet material compared to the DDM and the VM. However, the rated torque per kilogram of magnet material of the DDM, SMGM and RSMGM are more comparable. The VM achieved the highest torque per kilogram of magnet material, almost double that of the RSMGM.

The SMGM used the least amount of copper, followed by the DDM. The VM used the most copper, due to its use of overlap windings.

TABLE II
COMPARISON OF MACHINES.

Parameter	DDM	SMGM	RSMGM	VM	Unit
Gear stall torque	-	88.2	61.8	-	Nm
E_T	-	0.87	0.82	-	-
Rated torque (T)*	27.7	75.1	52.8	41.1	Nm
Rated stator torque	27.7	10.4	5.03	41.1	Nm
Stall torque density	-	114.6	80.3	-	kNm/m ³
Rated torque density	36.0	97.6	68.6	53.4	kNm/m ³
Gear ratio	-	7.2	10.5	11	-
End-winding factor	0.24	0.41	1.24	2.00	-
Rated copper loss	77.7	42.9	72.9	60.5	W
Magnet loss †	0.29	5.00	6.04	1.10	W
Core loss †	6.6	21.4	10.0	10.2	W
Total loss †	84.6	69.3	88.9	71.8	W
Frequency (150 rpm)	42.5	90	52.5	55	Hz
Efficiency (150 rpm)	80.6	94.2	89.3	88.9	%
Power factor	0.90	0.94	0.90	0.58	-
Magnet mass (M_m)	0.40	0.90	0.93	0.41	kg
Copper mass	1.61	1.14	2.12	3.91	kg
Steel mass	1.55	2.44	2.38	2.69	kg
Total active mass (M)	3.56	4.48	5.43	7.01	kg
Rated T/M_m	69.3	83.4	56.8	100.2	Nm/kg
Rated T/M	7.78	16.8	9.72	5.86	Nm/kg

* Rated torques of the two MGMs are based on a load angle $\delta_g = 60^\circ$.

† Based on 2D simulation data at 150 rpm and rated conditions

B. Operational Range

Figs. 11 - 16 compare the maximum output power characteristics of these machines over an operational speed range of 0 - 600 rpm. (Refer to Fig. 11 for legend.) In this comparison, only copper loss is considered which is the dominant loss mechanism in all cases. The number of turns of each machine was scaled such that the voltage limit of 400 V was reached at the base speed of 150 rpm, as can be seen in Fig. 11. The current limits, indicated by dashed lines in Fig. 12, were set such that the rated torque could be achieved at base speed. The current limits also indicate the relative VA-ratings of the power electronic drives of the respective machines, since the voltage limits are equal. The superior torque capability of the SMGM at low speeds can clearly be seen in Fig. 13. The RSMGM delivers more torque than the VM at low speed and uses an inverter with a lower VA-rating, but the VM can operate within the specified maximum voltage over a very wide speed range. The DDM can operate over a slightly wider speed range than the MGMs, but its torque and power capability is much lower than that of the other machines at low speeds.

The maximum output power of each machine, considering generator operation, is shown in Fig. 14. The peak power of the SMGM is very high. This graph shows that the vernier machine can deliver a relatively high constant power over a very wide speed range.

The efficiency of the SMGM is the highest. The RSMGM and the VM have similar efficiencies up to base speed. The efficiency of all three flux-modulating machines compare favourably with that of the DDM up to base speed. This analysis also shows that the VM can achieve high efficiency at higher speeds, although the plot shown here is a bit optimistic since core and magnet losses are not negligible in the higher speed region.

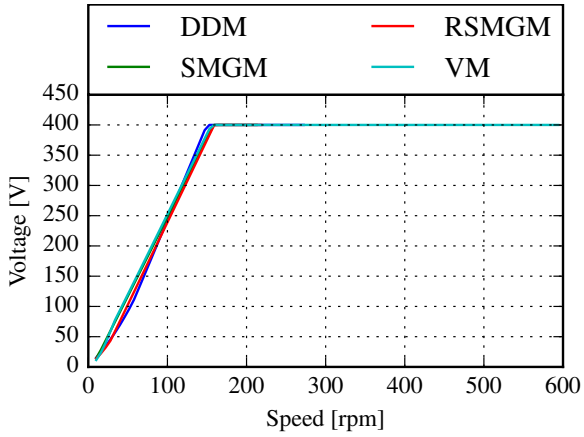


Fig. 11. Simulated line voltage comparison over operational speed range.

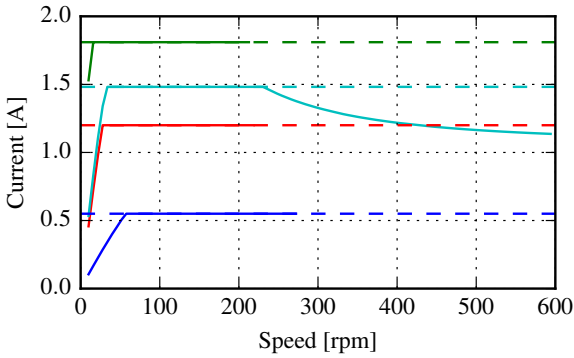


Fig. 12. Simulated phase current comparison over operational speed range.

The power factors of the four machines are compared in Fig. 16. The shape of these curves deserves an explanation. Consider, for example, the curve for the DDM: In the first part of the curve the current increases until it reaches a maximum value. As the current increases, the power factor drops. Then, in the second part of the curve, the current stays constant while the voltage increases up to its maximum value. In this section of the curve, the power factor increases due to improving efficiency. In the final section of the curve, both the voltage and current magnitudes stay constant at their maximum values. Initially, the output power and efficiency increases with a corresponding increase in power factor, but then the output power decreases and the power factor drops. The curves show that the two MGMs and the DDM can operate at high power factors over the major parts of their respective speed ranges. The VM has a poor power factor in the speed range where it delivers its maximum torque, but its power factor increases steadily until it reaches a high value at higher speeds.

C. Discussion of Machine Characteristics

In this section, the reasons for the differences in the performance characteristics of the machines are explored. The discussion is qualitative in nature.

The reason for the high torque capability of the MGMs lies in the high torque density of their incorporated magnetic

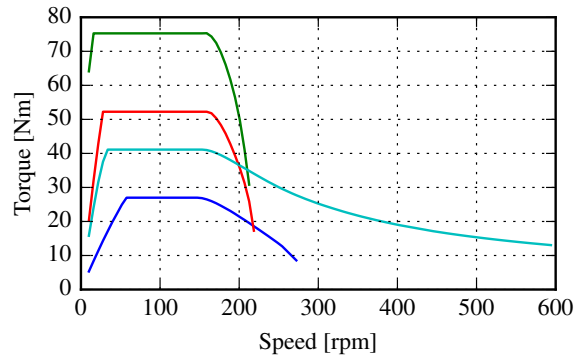


Fig. 13. Simulated torque comparison over operational speed range.

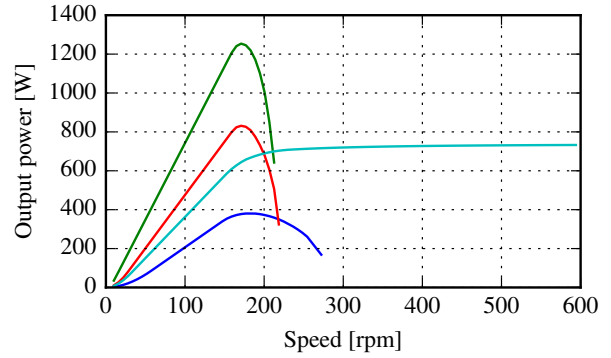


Fig. 14. Simulated output power comparison over operational speed range.

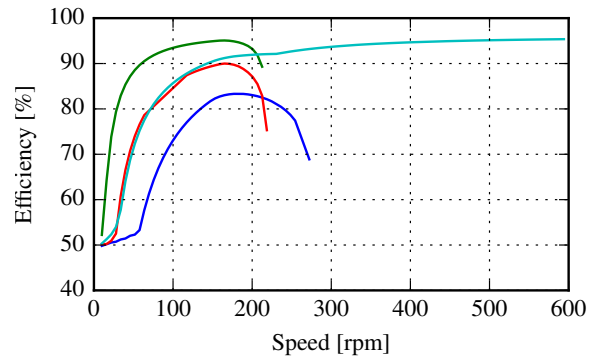


Fig. 15. Simulated efficiency comparison over operational speed range.

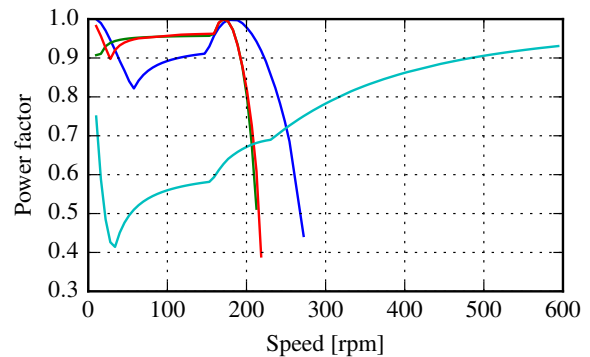


Fig. 16. Simulated power factor comparison over operational speed range.

gears. Magnetic gears, in turn, typically have a much higher torque density than electrical machines because a larger magnet volume can be leveraged within a confined space and because of the effectiveness of the flux modulation principle in generating high order air-gap flux density space harmonics. The SMGM performs better than the RSMGM because having an outer gear component with a larger diameter is advantageous for the size of machine considered in this paper. Furthermore, the closer coupling between the stator and the sun gear in the SMGM is advantageous. The fact that the tooth tips in the RSMGM have to act as a back yoke for the ring gear magnets is not desirable for two reasons: The yoke thickness is compromised and the closed slots result in large stator leakage flux, which weakens the coupling between the stator and the sun gear.

The poor power factor of the VM when it produces high torque is due to the low relatively low PM flux linkage in the machine. A larger portion of the air-gap flux is produced by the stator current. All the other machines considered here have high PM flux linkage and thus, good power factors. For the same reason, the VM achieves the highest torque per magnet volume. The low PM flux linkage is also the reason for the VM's wide operational speed range. The VM can achieve flux weakening not only by changing the current angle but also by simply reducing the current magnitude, as evidenced in Fig. 12.

The superior torque capability of the VM compared to the DDM is interesting because the machines are very similar, except for the winding layout. The flux modulation strategy appears to be more effective in producing the high order space harmonic than the non-overlap winding. Another factor is that the overlap winding layout combined with thin stator teeth allow a larger copper volume to be used effectively.

V. CONCLUSION

Permanent magnet machines based on flux-modulation can achieve high volumetric torque densities compared with more conventional fractional-slot PM machines. In this study, the split MGM achieved the highest volumetric torque density as well as the highest torque per mass. However, the construction of this topology poses significant challenges. The ring-stator MGM has a simpler mechanical structure and still outperforms the benchmark PM machine in terms of torque density and efficiency.

Importantly, it was found that the torque per magnet volume of the MGMs is comparable to that of the benchmark PM machine.

The vernier machine may be an attractive option since its performance is comparable to the ring-stator MGM in terms of torque density and efficiency, yet it has a simple structure. Furthermore, the vernier machine achieved the highest torque per volume of magnet material, which may make it a cost effective alternative where high power factor is not critical.

The comparisons made in this paper clearly demonstrate some of the advantages associated with flux-modulating electrical machines. However, the study considered small

machines with rated powers in the range of 1 kW. Further comparisons at higher power levels are required.

REFERENCES

- [1] K. Chau, D. Zhang, J. Jiang, C. Liu, and Y. Zhang, "Design of a Magnetic-Geared Outer-Rotor Permanent-Magnet Brushless Motor for Electric Vehicles," *IEEE Trans. Magn.*, vol. 43, no. 6, pp. 2504–2506, 2007.
- [2] K. Atallah, J. Rens, S. Mezani, and D. Howe, "A Novel 'Pseudo' Direct-Drive Brushless PM Machine," *IEEE Trans. Magn.*, vol. 44, no. 11, pp. 4349–4352, 2008.
- [3] P. Rasmussen, H. H. Mortensen, T. Matzen, T. Jahns, and H. Toliyat, "Motor integrated permanent magnet gear with a wide torque-speed range," in *IEEE Energy Conv. Congress & Expo. (ECCE)*, 2009, pp. 1510–1518.
- [4] S. Mezani, T. Hamiti, L. Belguerras, T. Lubin, M. Rashed, and C. Gerada, "Magnetically Geared Induction Machines," *IEEE Transactions on Magnetics*, vol. 51, no. 11, pp. 1–4, Nov. 2015.
- [5] M. Johnson, M. C. Gardner, and H. A. Toliyat, "Design and Analysis of an Axial Flux Magnetically Geared Generator," *IEEE Transactions on Industry Applications*, vol. 53, no. 1, pp. 97–105, Jan. 2017.
- [6] M. B. Kouhshahi, J. Z. Bird, V. Acharya, K. Li, M. Calvin, and W. Williams, "An axial flux-focusing magnetically geared motor," in *2017 IEEE Energy Conversion Congress and Exposition (ECCE)*, Oct. 2017, pp. 307–313.
- [7] D. Li, R. Qu, and J. Li, "Topologies and analysis of flux-modulation machines," in *2015 IEEE Energy Conversion Congress and Exposition (ECCE)*, Sep. 2015, pp. 2153–2160.
- [8] J. Li, K. T. Chau, J. Z. Jiang, C. Liu, and W. Li, "A New Efficient Permanent-Magnet Vernier Machine for Wind Power Generation," *IEEE Transactions on Magnetics*, vol. 46, no. 6, pp. 1475–1478, Jun. 2010.
- [9] D. Li, R. Qu, and T. A. Lipo, "High-Power-Factor Vernier Permanent-Magnet Machines," *IEEE Transactions on Industry Applications*, vol. 50, no. 6, pp. 3664–3674, Nov. 2014.
- [10] G. Xu, G. Liu, M. Chen, X. Du, and M. Xu, "Cost-Effective Vernier Permanent-Magnet Machine With High Torque Performance," *IEEE Transactions on Magnetics*, vol. 53, no. 11, pp. 1–4, Nov. 2017.
- [11] S. Gerber and R. J. Wang, "Torque capability comparison of two magnetically geared PM machine topologies," in *2013 IEEE International Conference on Industrial Technology (ICIT)*, Feb. 2013, pp. 1915–1920.
- [12] —, "Design and evaluation of a PM vernier machine," in *2015 IEEE Energy Conversion Congress and Exposition (ECCE)*, Sep. 2015, pp. 5188–5194.
- [13] —, "Design and Evaluation of a Magnetically Geared PM Machine," *IEEE Trans. Magn.*, vol. 51, no. 8, pp. 1–10, Aug. 2015.
- [14] P. M. Tlali, S. Gerber, and R. J. Wang, "Optimal Design of an Outer-Stator Magnetically Geared Permanent Magnet Machine," *IEEE Trans. Magn.*, vol. 52, no. 2, pp. 1–10, Feb. 2016.
- [15] S. Gerber and R. J. Wang, "Analysis of the end-effects in magnetic gears and magnetically geared machines," in *2014 International Conference on Electrical Machines (ICEM)*, Sep. 2014, pp. 396–402.

Stiaan Gerber (M'13) was born in Bellville in South Africa on February 20, 1986. He received his PhD in Electrical Engineering at Stellenbosch University in 2015 where he is currently working as a postdoctoral researcher. His main interests in the engineering field are electrical machine design, numerical optimization, renewable energy power generation and finite element methods.

Rong-Jie Wang (M'00–SM'08) received the MSc(Eng) degree from the University of Cape Town in 1998 and the PhD(Eng) degree from Stellenbosch University in 2003, all of South Africa. He has been affiliated with the Department of Electrical and Electronic Engineering of Stellenbosch University since 2003, where he is currently an Associate Professor. His research interests include special electrical machines, computer-aided design and optimization of electrical machines, computational electromagnetics, thermal modeling of electrical machines and renewable energy systems. He was a co-author of the monograph *Axial Flux Permanent Magnet Brushless Machines* (2nd ed., Springer 2008).